

## 1 **Effect of Potassium Hydroxide Concentration and Activation Time on Rice Husk-Activated Carbon** 2 **for Water Vapor Adsorption**

3 Dewi Qurrota A'yuni<sup>1</sup>, Hadianono<sup>1</sup>, Velny<sup>1</sup>, Agus Subagio<sup>2</sup>, Moh. Djaeni<sup>1,\*</sup> and Nandang Mufti<sup>3</sup>

4 <sup>1</sup>*Department of Chemical Engineering, Faculty of Engineering, Universitas Diponegoro*

5 <sup>2</sup>*Department of Physics, Faculty of Science and Mathematics, Universitas Diponegoro Jl. Prof. Soedarto*  
6 *Tembalang, Semarang, Central Java, Indonesia 50275*

7 <sup>2</sup>*Department of Physics, Faculty of Mathematics and Science, Universitas Negeri Malang Jl. Semarang*  
8 *No.5, Sumber Sari, Lowokwaru, Malang, East Java 65145*

9 *\*Corresponding Author e-mail: moh.djaeni@live.undip.ac.id*

10  
11 **Abstract:** Rice husk carbon by-product from the industrial combustion is a promising source to produce a  
12 vast amount of activated carbon adsorbent. This research prepared rice husk-activated carbon adsorbent by  
13 varying the concentration of potassium hydroxide solution (5, 10, 15, 20 % w/v) and activation time (2, 4,  
14 6, 8 hours). Fourier-transform infrared spectral characterization (FTIR) indicated a significant effect before  
15 and after activation, especially the presence of hydroxyl groups. Based on the iodine adsorption, the specific  
16 surface area of the produced-activated carbon was approximately 615 m<sup>2</sup>/g. Experimental results showed  
17 that increasing potassium hydroxide concentration and activation time increases the water vapor adsorption  
18 capacity of the activated carbon. Compared with the rice husk carbon, the KOH-activated carbon enhanced  
19 the water vapor adsorption capacity to 931%. In the adsorption observation, changing the temperature from  
20 15 to 27 °C caused a higher water vapor uptake onto the activated carbon. Two adsorption kinetics (pseudo-  
21 first- and pseudo-second-order models) were used to evaluate the adsorption mechanism. This research  
22 found that rice husk-activated carbon performed a higher water vapor adsorption capacity than other  
23 adsorbents (silica gel, zeolite, and commercially activated carbon).

24 **Keywords:** *activated carbon, adsorption kinetics, desiccant, rice husk, water vapor adsorption*

## 25 INTRODUCTION

26 Water vapor adsorption is an essential process in several industrial practices, such as water harvesting [1],  
27 dehumidification [2], and desalination. As an example, in the dehumidification drying process, reducing  
28 water vapor from air enhances the driving force, which can shorten the drying time and retain heat-  
29 sensitive ingredients in the food product [3]. This is due to the significant difference between the  
30 concentration of water vapor on the food's surface and the air as the drying medium. Then, the mass  
31 transfer of water vapor from the product to the air can be fastened.

32 The need for water vapor adsorption led to the production of efficient materials for moisture control.  
33 Some studies presented different types of water adsorbents, including Covalent Organic Frameworks [4],  
34 Metal-Organic Frameworks (MOFs) [5], zeolite [6], silica gel [7], mesoporous silica [8], and activated  
35 carbon [9]. Covalent Organic Frameworks (COFs) and Metal-Organic Frameworks (MOFs) are mostly  
36 used in the water harvesting process because of their remarkable adsorption properties, which are highly  
37 tunable and high porosity [10]. However, those materials require careful handling due to potential  
38 structural damage and complex synthesis processes, making them relatively higher cost compared to other  
39 adsorbents [11]. Meanwhile, widely known water vapor adsorbents or desiccants (zeolite, silica gel, and  
40 activated carbon) are easily regenerated and more stable in structure.

41 There are several requirements in the adsorbent selection, including toxicity, adsorption capacity, cycles,  
42 and easiness in regeneration using low heat energy. Activated carbon is a non-toxic and thermally stable  
43 adsorbent with a high water adsorption capacity due to its large surface area [12]. Also, activated carbon  
44 can be produced from natural sources such as agricultural by-products. Thus, activated carbon is a  
45 promising adsorbent due to its abundance, low cost, and potential for sustainable water vapor removal.

46 Rice husk is a natural adsorbent that has been applied for various applications, including heavy metal and  
47 dye removal in wastewater [13], [14], CO<sub>2</sub> adsorption [2], and urine purification [15]. In its application as  
48 a water vapor adsorbent, rice husk was exploited by Warsiki et al. [16] that produce rice husk-CaCl<sub>2</sub>  
49 composite desiccant. They reported that environmental humidity (water activity) and temperature  
50 influenced the adsorption capacity of the adsorbent. However, the study did not compare rice husk-CaCl<sub>2</sub>

51 adsorption with other adsorbents. Moreover, untreated rice husk still contains contaminants in its pores  
52 and thus is still low in adsorption capacity. Another research showed that rice husk silica had the potential  
53 as a silica gel substitute in water vapor adsorption [17]. The adsorption mechanism of rice husk silica and  
54 silica gel was similar and affected by silanol groups on their surface. Nevertheless, commercial silica  
55 adsorbed twice as much water vapor than silica produced from rice husk. Therefore, this research focuses  
56 on synthesizing natural-based adsorbent with high water vapor adsorption.

57 This work aims to produce activated carbon from rice husk as a water vapor adsorbent and its comparison  
58 with other commercial adsorbents (commercial activated carbon, silica gel, and zeolite). In the process,  
59 several studies used potassium hydroxide, zinc chloride, hydrochloric acid, and sodium hydroxide as  
60 activation agents to activate rice husk carbon [18], [19], [20]. In this study, potassium hydroxide (KOH)  
61 was selected as the activation agent to increase the pore volume and adsorption capacity of the adsorbent  
62 water vapor [21]. The activation agent concentration and the activation time were studied to assess the  
63 water vapor adsorption property.

## 64 **EXPERIMENTAL PROCEDURE**

### 65 **Materials**

66 Rice husk char was bought from a local shop in Pedurungan, Semarang, Central Java. The char was sun-  
67 dried before being activated. The experiment was conducted using potassium hydroxide (90% purity,  
68 technical grade), hydrochloric acid (concentration of 32%, technical grade), distilled water, iodine solution  
69 (concentration of 1%, Merck & Co., Inc.), sodium thiosulfate (98% purity, Merck & Co., Inc.), and  
70 amylum (99% purity, Merck & Co., Inc.). Commercial adsorbents that were used as a comparison were  
71 coal-based commercial activated carbon (size of 4 – 8 mesh), white silica gel (size of 2 – 4 mm), and  
72 natural zeolite bought from a local shop (CV. Indrasari, Semarang, Central Java).

### 73 **Carbon Activation**

74 Before activation, rice husk char was prepared by pulverizing and sieving to 20 and 25 mesh. Char  
75 activation was conducted by adding 25 grams of rice husk char to 150 mL of 5% w/v KOH solution and

76 letting it stand for 8 hours. The activated char (activated carbon) was filtered and washed using HCl and  
77 distilled water until the washing solution achieved a neutral pH. The wet activated carbon was dried in an  
78 oven at 110°C to the achievement of a constant mass and was placed in a desiccator. The activation  
79 procedure was repeated using KOH solution at different concentrations (10, 15, and 20% w/v) and  
80 activation times (2, 4, and 6 hours).

### 81 Iodine Number Adsorption

82 The iodine adsorption experiment was begun by mixing the activated carbon and 0.1 N iodine solution for  
83 10 minutes. After the filtration, 10 mL of filtrate was titrated with 0.1 N sodium thiosulfate ( $\text{Na}_2\text{S}_2\text{O}_3$ )  
84 until became light yellow. The solution was then titrated by 1% amylum until clear from the blue color.  
85 The iodine adsorption capacity was calculated by the equation of (Sulistyah et al., 2020)

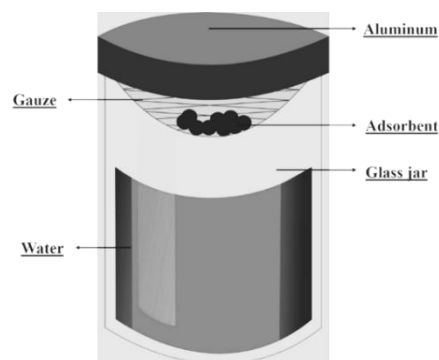
$$\text{Iodine number} = \frac{(V_1N_1 - V_2N_2)126.9 \times 5}{W} \quad (1)$$

86 with  $V_1$  and  $V_2$  are volume of iodine and sodium thiosulfate (mL), respectively,  $N_1$  is the normality of  
87 iodine (N),  $N_2$  normality of sodium thiosulfate (N), and  $W$  is the mass of the sample (g).

### 88 Adsorption capacity

89 Fig. 1 describes the experimental setup of the adsorption test. The adsorption capacity of the produced  
90 activated carbon was evaluated by placing 10 grams of activated carbon in an isolated mason jar.

91 Previously, the jar was filled with a specific amount of water. The adsorption capacity was the total mass  
92 of water adsorbed into the sample that was measured by the gravimetric method. This test was conducted  
93 under temperatures of 15 °C, room temperature (27 °C), and 40 °C for several days until equilibrium. In  
94 comparison, several commercial adsorbents were also examined with iodine and water vapor adsorption.  
95 The adsorption kinetics was evaluated using several models presented in Table 1. The adsorption capacity  
96 of prepared activated carbon was then compared to other commercial adsorbents (commercial activated  
97 carbon, natural zeolite, and silica gel).



98  
99 Fig. 1. Experimental set-up of the adsorption capacity evaluation

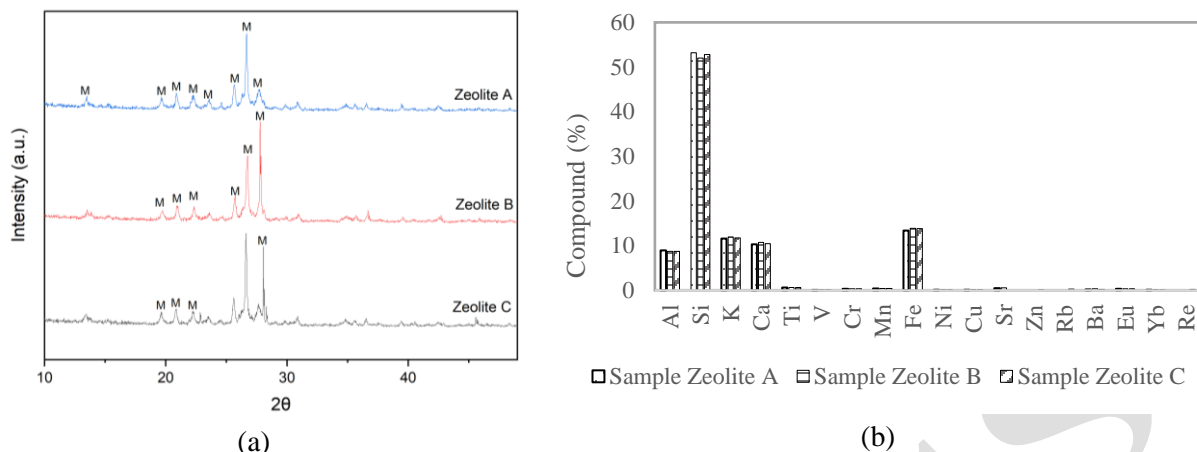
100 Table 1. Adsorption kinetics equation (Gurses et al. 2006; Qiu et al. 2009)

Model	Equation
Pseudo-first-order	$q_t = q_e(1 - e^{-k_1 t})$
Pseudo-second-order	$q_t = \frac{k_2 q_e^2 t}{1 + k_2 q_e t}$

Notes:  $q_t$  = moisture adsorption at a certain time;  $q_e$  = moisture adsorption at equilibrium;  $t$  = adsorption time;  $k_1$  = constant parameter of pseudo-first-order;  $k_2$  = constant parameter of pseudo-second-order

### 101 Materials Characterization

102 The functional groups in the activated carbon samples were examined using Fourier Transform Infrared  
 103 Spectroscopy (FTIR) employing PerkinElmer Frontier Infrared Spectrometer version 10.6.1, with a  
 104 resolution of  $1 \text{ cm}^{-1}$  in a region of  $400$  to  $4000 \text{ cm}^{-1}$ . X-ray diffractions (XRD PANalytical X'Pert PRO,  
 105 Malvern Panalytical Ltd.) with  $\text{CuK}\alpha$  radiation of  $1.54060 \text{ \AA}$  were used to investigate the crystallinity of  
 106 natural zeolite. This instrument operated at  $40 \text{ kV}$ ,  $30 \text{ mA}$  and the diffractograms were observed from  
 107  $10.03^\circ$  to  $82.19^\circ$  on a  $2\theta$  scale with a  $0.7^\circ$  step size. The chemical compositions of natural zeolite were  
 108 observed using X-ray Fluorescence (Panalytical Minipal 4, Malvern Panalytical Ltd.). Three random  
 109 samples were taken from the same source as the zeolite samples, named Zeolite A, B, and C. The crystal  
 110 structure and the chemical composition of natural zeolite were shown in XRD patterns and XRF analysis  
 111 in Fig. 2. According to XRD patterns evaluated by Highscore plus 3.0e (PANalytical B.V., The  
 112 Netherlands), the peaks of zeolite samples indicate similar crystal structure (mordenite). This result was  
 113 compatible with XRF analysis that showed a common compound of mordenite mineral ( $\text{Na}_2$ ,  $\text{Ca}$ ,  $\text{K}_2$ )  
 114  $\text{Al}_2\text{Si}_{10}\text{O}_{24} \cdot 7\text{H}_2\text{O}$  [22].

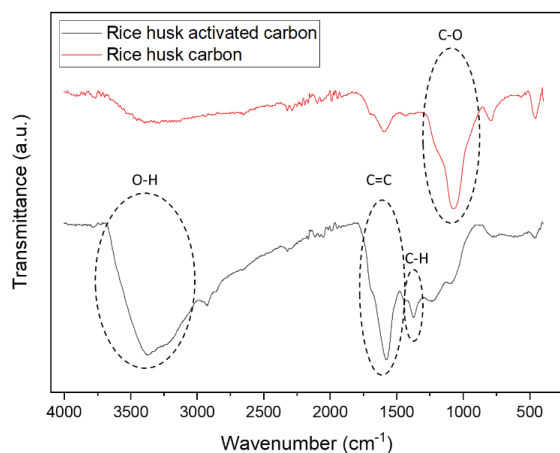


115 Fig. 2. (a) XRD patterns of natural zeolite used in this study (b) compounds found in natural zeolite used  
 116 in this study

## 117 Results and Discussion

### 118 Fourier transform infrared (FTIR) characterization

119 Fig. 3 shows the FTIR spectra of rice husk char and activated carbon, which highlight the chemical  
 120 functional groups. Several functional groups with water affinity were discovered by this characterization,  
 121 as well as some water that had bound to the activated carbon. A clear difference between the two samples  
 122 was a higher peak of aromatic ring C=C at  $1600 - 1500 \text{ cm}^{-1}$  in the activated carbon and a C-O band of  
 123 rice husk char at  $1300 - 1050 \text{ cm}^{-1}$  [23]. A C-H functional group at a wavenumber of  $1374 \text{ cm}^{-1}$   
 124 corresponds to bending vibrations in methyl groups [24]. It also found a higher broad peak in the range of  
 125 wavenumber of  $3600 - 3200 \text{ cm}^{-1}$ , representing the O-H functional group and indicating the moisture-  
 126 enriched surface of the activated carbon [13]. The oxygen-containing functional groups had the ability to  
 127 fasten the water vapor adsorption performance of the activated carbon [24].



128

129 Fig. 3. FTIR spectra of rice husk char and activated carbon

130 **Iodine Adsorption**

131 According to Mianowski et al. [25], iodine adsorption can represent the surface area of activated carbon

132 for a range of 200 – 850 mg/g iodine number. Therefore, the surface area of rice husk activated carbon in

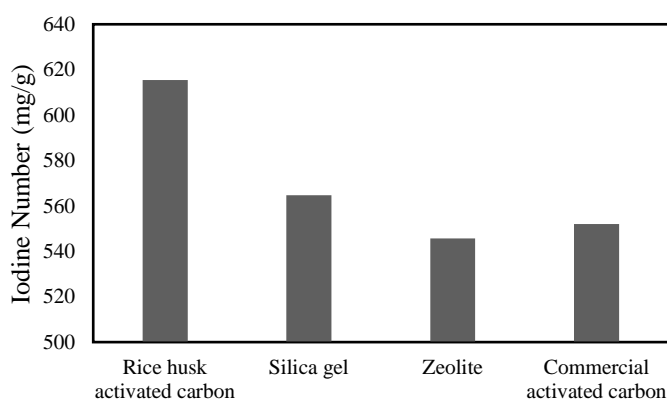
133 this study was around 615 m<sup>2</sup>/g and higher than other tested commercial adsorbents (Fig. 4). According to

134 this result, the product can be potentially developed as a high-capacity water vapor adsorbent. However,

135 this result was still lower than nano-porous carbon with iodine adsorption of more than 700 mg/g [20].

136 This result indicates that the activated carbon product from this experiment had a higher lack of well-

137 developed porosity than that of nano-porous carbon from rice husk.

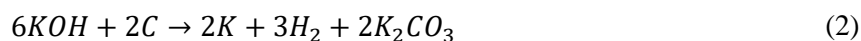


138

139 Fig. 4. Iodine adsorption of several adsorbents

#### 140 **Effect of potassium hydroxide concentration**

141 In the activation stage, the chemical reaction that occurred was [26]

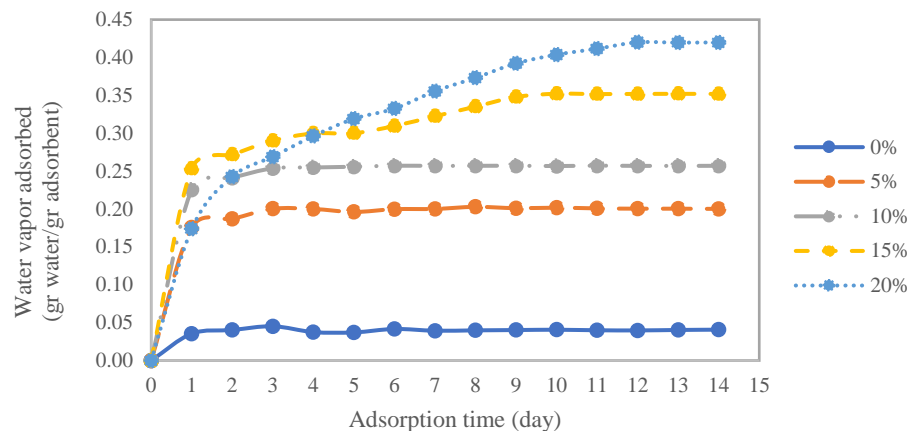


142 Based on the reactions, KOH and carbon decomposed into potassium compounds (K and  $K_2CO_3$ ) and  
143 hydrogen. The activated carbon was then washed with acid and water to remove them, clearing carbon  
144 pores [27]. Therefore, the water vapor adsorption of carbon was increased after the activation (Fig. 5).

145 Untreated rice husks possessed the lowest adsorption capacity (0.04 g water/g adsorbent). Fig. 5 also  
146 presents water vapor adsorption of the activated carbon that was treated using different KOH  
147 concentrations for 8 hours. The data shows that manufacturing activated carbon using higher KOH  
148 concentration impacted a higher adsorption capacity. The highest adsorption capacity (0.42 g vapor/g  
149 adsorbent) belonged to activated carbon obtained from activation using 20% w/v KOH solution, and the  
150 lowest was found at 5% w/v KOH solution.

151 This finding confirmed the FTIR characterization that showed a hydroxyl functional group on the  
152 activated carbon. Also, the theory stated that a higher activation agent concentration facilitates higher  
153 carbon degradation to produce more pores [28]. However, the produced activated carbon was still lower  
154 than activated carbon derived from coffee shells [24] and tobacco stems [29]. The significance of different  
155 concentrations and adsorption times were evaluated with ANOVA summarized in Table 2, showing a  
156 significant impact of both factors (p-value < 0.05).





157  
 158 Fig. 5. Water vapor adsorption of activated carbon at different concentrations  
 159 Table 2. Two-way ANOVA of water vapor adsorption of the activated carbon at different adsorption times  
 160 and KOH concentrations

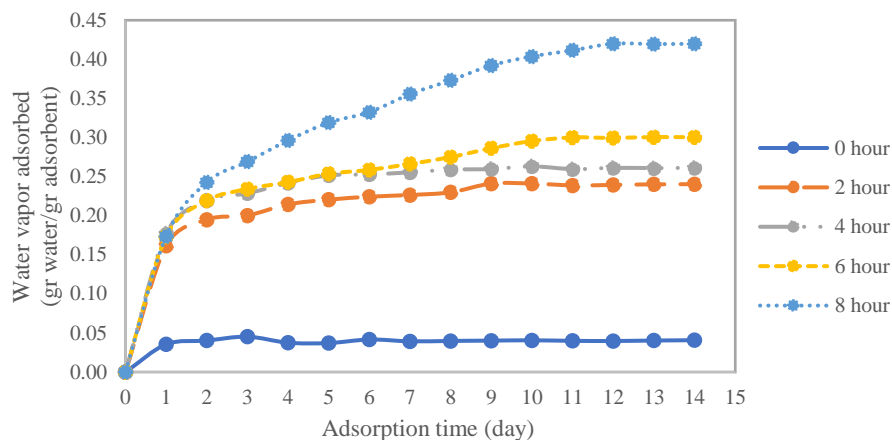
Source of Variation	SS	df	MS	F	P-value	F crit
Adsorption time	28.9739	14	2.0696	10.7222	< 0.001	1.8726
Concentration	77.3276	4	19.3319	100.1570	< 0.001	2.5366
Error	10.8089	56	0.1930			
Total	117.1103	74				

### 161 Effect of Activation Time

162 The analysis of the activation time was conducted for activated carbon that was activated using 20% w/v  
 163 KOH solution for 2 – 8 hours. Fig. 6 depicts the adsorption capacity at different activation times. The  
 164 highest adsorption capacity was achieved at 8 hours of carbon activation (0.420 g vapor adsorbed/g  
 165 adsorbent). Compared to the untreated rice husk char, activating the carbon for 8 hours increased the  
 166 adsorption capacity up to 9 times. Analysis of the variance of this result also demonstrated that varying the  
 167 activation period has a significant effect on the adsorption capacity (Table 3).

168 Previous studies reported a different relationship between the activation time and adsorption capacity [24],  
 169 [28]. Sun et al. [24] stated that changes in activation time did not have a significant effect on the  
 170 maximum adsorption capacity. In contrast, Yang et al. [28] found a fluctuation in the adsorption capacity  
 171 of activated carbon at different activation times. From a range of 0.5 to 3.0 hours, the maximum  
 172 methylene blue adsorption was at 2 hours. That result occurred because of an excessive increase in

173 reaction rate between KOH and carbon causing a higher growth of porous structure. Extending the  
 174 activation duration can increase the contaminants degradation and maximize the microporous formation  
 175 [30].



176

177 Fig. 6. Water vapor adsorption capacities at different activation times

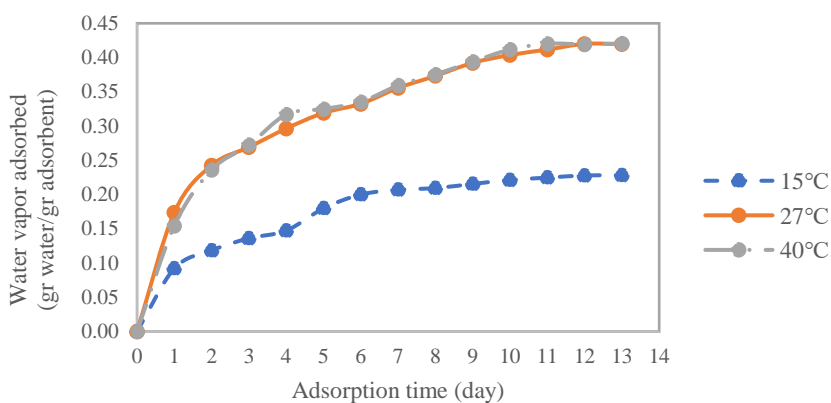
178 Table 3. Two-way ANOVA of water vapor adsorption of the activated carbon at different activation times

Source of Variation	SS	df	MS	F	<i>P-value</i>	F crit
Adsorption time	30.0561	14	2.1469	13.3901	< 0.001	1.8726
Activation time	66.2628	4	16.5657	103.3209	< 0.001	2.5366
Error	8.9786	56	0.1603			
Total	105.2976	74				

179 **Effect of Adsorption Temperature**

180 The effect of adsorption temperature on the water vapor adsorption capacity of activated carbon was  
 181 presented in Fig. 7. The test observed that a change of temperature of 15 °C to 27 °C affected the  
 182 adsorption capacity. At 40 °C, there was no significant difference in the maximum water vapor adsorption  
 183 capacity. More details, ANOVA indicated that the adsorption temperature and time had a significant effect  
 184 on the water vapor adsorption (Table 4). Before, Chairunnisa et al. [12] and Cardenas et al. [31] explored  
 185 the water vapor adsorption of activated carbon at 20 - 40°C. They found that increasing the adsorption  
 186 temperature caused a reduction in the adsorption capacity. Combined with our results, the phenomenon  
 187 that happened was a rapid formation of water clusters at temperatures lower than 30°C, and at higher

188 temperatures, this water cluster became less stable [12]. Higher temperatures sped up the movement of  
 189 water molecules and reduced the attraction of adsorbent and water [32].



190

191 Fig. 7. Water vapor adsorption capacity at different temperatures

192 Table 4. Two-way ANOVA of water vapor adsorption capacity of the activated carbon at different

193 temperatures

Source of Variation	SS	df	MS	F	<i>P-value</i>	F crit
Time	0.3975	13	0.0306	31.5170	< 0.001	2.1192
Temperature	0.1939	2	0.0970	99.9622	< 0.001	3.3690
Error	0.0252	26	0.0010			
Total	0.6166	41				

194

195 Fig. 8 displays the effect of the adsorption temperature of several adsorbents. Interestingly, different  
 196 adsorbents exhibited a different relationship. For example, when the temperature increased from 15 °C to  
 197 40 °C, the maximum adsorption capacity of commercial activated carbon decreased by 33%. Furthermore,  
 198 the adsorption capacity of other adsorbents increased when the temperature increased from 15°C to 40°C.  
 199 Also, this comparison indicated that the produced activated carbon from rice husk adsorbed more water  
 200 vapor than other tested commercial adsorbents. This result was in agreement with the iodine adsorption  
 201 test that showed a higher surface area of rice husk-activated carbon than other adsorbents.

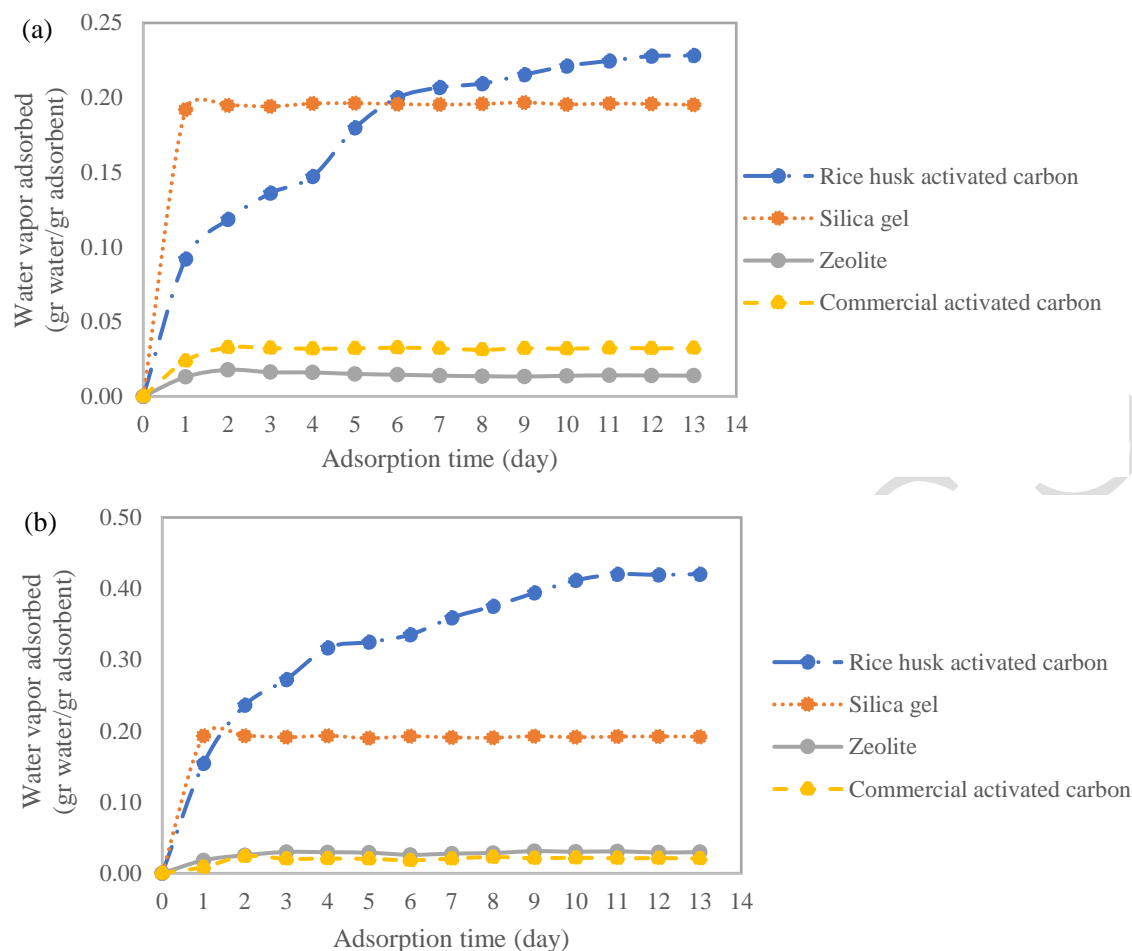


Fig. 8. Water vapor adsorption of several adsorbents at temperatures of (a) 15°C, (b) 40°C

### Adsorption Kinetics

The adsorption kinetics of prepared activated carbon (20% w/v KOH solution and 8 hours activation) was evaluated by pseudo-first- and pseudo-second-order models. The kinetic study was analyzed by varying the adsorption temperature at 15 °C, 27 °C, and 40 °C. The parameters of the two models are provided in Table 5. The most suitable model was determined by coefficient of determination ( $R^2$ ) and SSE. Based on the calculation, two models show good fits with  $R^2$  close to 1.0 and SSE close to 0. Furthermore, the pseudo-first-order model described the adsorption mechanism of activated carbon prepared at the highest concentration and longest activation time was better than the second-order ( $R^2$  values closer to 1 and SSE closer to 0). It implied that the main mechanism for the adsorption of water vapor on that activated carbon was physisorption. Meanwhile, the pseudo-second-order model described some samples better than the

202

203

204

205

206

207

208

209

210

211

212

213

214

215 first-order, agreeing to the chemisorption process [33].

216 Table 5. Parameters of non-linear pseudo-first- and pseudo-second-order model

Concentration (% w/v)	Pseudo-First-Order				Pseudo-Second-Order			
	$k_1$	$q_e$	$R^2$	SSE	$k_2$	$q_e$	$R^2$	SSE
5	0.0013	0.2001	0.8383	$9.6 \times 10^{-6}$	0.0240	0.2001	0.8921	$1.9 \times 10^{-5}$
10	0.0009	0.2572	0.9396	$6.3 \times 10^{-5}$	0.0714	0.2569	0.9551	$4.5 \times 10^{-5}$
15	0.0005	0.3506	0.6702	0.0008	0.0034	0.3506	0.8340	0.0002
20	0.0002	0.4184	0.9618	0.0006	0.0012	0.4184	0.9492	0.0007
Activation time (hour)								
2	0.0003	0.2405	0.9614	0.0006	0.0078	0.2405	0.9561	$6.0 \times 10^{-5}$
4	0.0003	0.2656	0.9864	0.0008	0.0062	0.2656	0.9905	$3.0 \times 10^{-5}$
6	0.0003	0.3013	0.8805	0.0005	0.0031	0.3013	0.9309	0.0001
8	0.0002	0.4184	0.9613	0.0006	0.0010	0.4184	0.9532	0.0008
Temperature (°C)								
15	0.0002	0.2326	0.9686	0.0001	0.0019	0.2326	0.9398	0.0003
27	0.0002	0.4184	0.9613	0.0006	0.0010	0.4184	0.9532	0.0008
40	0.0003	0.4224	0.9425	0.0007	0.0009	0.4224	0.9772	0.0011

## 217 CONCLUSION

218 Activated carbon from rice husks was activated by varying the concentration of KOH as the activation  
 219 agent and the activation time. The Fourier transform infrared (FTIR) spectral characterization represents  
 220 that there was a significant effect on the activation of rice husk activated carbon as indicated by  
 221 differences in functional groups before and after activation, including the addition of the hydroxyl group  
 222 which made the activated carbon more hydrophilic, and the presence of the C=C group indicated an  
 223 increase in carbon content. Based on the iodine adsorption test, the surface area of the activated carbon  
 224 produced was around  $615 \text{ m}^2/\text{g}$ . The adsorption test showed that an increase in KOH concentration of up  
 225 to 20% (w/v) and an activation time of 8 hours could increase the adsorption capacity of the resulting  
 226 activated carbon (up to  $0.420 \text{ g/g}$ ). Adsorption was also examined at  $15^\circ\text{C}$ ,  $27^\circ\text{C}$ , and  $40^\circ\text{C}$  and showed  
 227 an increase in adsorption capacity with increasing temperature. The produced activated carbon that was  
 228 activated using 20% w/v KOH for 8 hours showed a good fit with the pseudo-first-order adsorption  
 229 kinetics model. According to the comparison, activated carbon from rice husk showed a higher adsorption

230 capacity than silica gel, zeolite, and commercial activated carbon. This research found that activated  
231 carbon from rice husks is a promising material to be applied to the dehumidification system of a drying  
232 process.

### 233 ACKNOWLEDGEMENT

234 This research was funded by Diponegoro University contract number 118-24/UN7.6.1/PP-22.

### 235 REFERENCES

- 236 [1] Sleiti, A. K., Al-Khawaja, H., Al-Khawaja, H. and Al-Ali, M., “*Harvesting Water from Air Using*  
237 *Adsorption Material – Prototype and Experimental Results.*” *Sep. Purif. Technol.*, 2021, 257,  
238 117921.
- 239 [2] Wang, C., Yang, B., Ji, X., Zhang, R. and Wu, H., “*Study on Activated Carbon/Silica Gel/Lithium*  
240 *Chloride Composite Desiccant for Solid Dehumidification.*” *Energy*, 2022, 251, 123874.
- 241 [3] Djaeni, M. and Perdanianti, A. M., “*The Study Explores the Effect of Onion (Allium Cepa L.)*  
242 *Drying Using Hot Air Dehumidified by Activated Carbon, Silica Gel and Zeolite.*” *J. Phys.: Conf.*  
243 *Ser.*, 2019, 1295, 012025.
- 244 [4] Xia, X., Liu, Z. and Li, S., “*Adsorption Characteristics and Cooling/Heating Performance of COF-*  
245 *5.*” *Appl. Therm. Eng.*, 2020, 176, 115442.
- 246 [5] Ashraf, S., Sultan, M., Bahrami, M., McCague, C., Shahzad, M. W., Amani, M., Shamshiri, R. R.  
247 and Ali, H. M., “*Recent Progress on Water Vapor Adsorption Equilibrium by Metal-Organic*  
248 *Frameworks for Heat Transformation Applications.*” *Int. Commun. Heat and Mass Transf.*, 2021,  
249 124, 105242.
- 250 [6] Moura, P. A. S., Rodríguez-Aguado, E., Maia, D. A. S., Melo, D. C., Singh, R., Valencia, S.,  
251 Webley, P. A., Rey, F., Bastos-Neto, M., Rodríguez-Castellón, E. and Azevedo, D. C. S., “*Water*  
252 *Adsorption and Hydrothermal Stability of CHA Zeolites with Different Si/Al Ratios and*  
253 *Compensating Cations.*” *Catal. Today*, 2022, 390–391, 99–108.

- 254 [7] Zheng, X., Chen, K. and Lin, Z., “*Synthesis and Characterization of Alginate–Silica Gel*  
255 *Composites for Adsorption Dehumidification.*” *Ind. Eng. Chem. Res.*, 2020, 59, 5760–5767.
- 256 [8] A’yuni, D. Q., Subagio, A., Hadiyanto, H., Kumoro, A. C. and Djaeni, M., “*Microstructure Silica*  
257 *Leached by NaOH from Semi-Burned Rice Husk Ash for Moisture Adsorbent.*” *Arch. Mater. Sci.*  
258 *Eng.*, 2021, 1, 5–15.
- 259 [9] Sun, S., Yu, Q., Li, M., Zhao, H., Wang, Y. and Ji, X., “*Effect of Carbonization Temperature on*  
260 *Characterization and Water Vapor Adsorption of Coffee-Shell Activated Carbon.*” *Ads. Sci.*  
261 *Technol.*, 2020, 38, 377–392.
- 262 [10] Zu, K. and Qin, M., “*Experimental and Modelling Investigation of Water Adsorption of Hydrophilic*  
263 *Carboxylate-Based MOF for Indoor Moisture Control.*” *Energy*, 2021, 228, 120654.
- 264 [11] Gargiulo, N., Peluso, A. and Caputo, D., “*MOF-Based Adsorbents for Atmospheric Emission*  
265 *Control: A Review.*” *Processes*, 2020, 8, 613.
- 266 [12] Chairunnisa, Miksik, F., Miyazaki, T., Thu, K., Miyawaki, J., Nakabayashi, K., Wijayanta, A. T.  
267 and Rahmawati, F., “*Development of Biomass Based-Activated Carbon for Adsorption*  
268 *Dehumidification.*” *Energy Rep.*, 2021, 7, 5871–5884.
- 269 [13] Liu, Z., Sun, Y., Xu, X., Qu, J. and Qu, B., “*Adsorption of Hg(II) in An Aqueous Solution by*  
270 *Activated Carbon Prepared from Rice Husk Using KOH Activation.*” *ACS Omega*, 2020, 5, 45,  
271 29231–29242.
- 272 [14] Wazir, A. H., Ullah, I. and Yaqoob, K., “*Chemically Activated Carbon Synthesized from Rice Husk*  
273 *for Adsorption of Methylene Blue in Polluted Water.*” *Environ. Eng. Sci.*, 2023, 40, 307–317.
- 274 [15] Sintawardani, N., Adhilaksma, C. A., Hamidah, U., Pradanawati, S. A. and Suharno, S. M.,  
275 “*Evaluation of Human Urine Purification Using Rice Husk Charcoal as The Adsorbent.*” *IOP Conf.*  
276 *Ser.: Earth Environ. Sci.*, 2023, 1201, 012107.
- 277 [16] Warsiki, E., Agriawati, D., Noor, E. and Iskandar, A., “*Isotherm Moisture Sorption of Composite*  
278 *Desiccant Made from Rice Husk Biomass.*” *IOP Conf. Ser.: Earth Environ. Sci.*, 2021, 749, 012011.

- 279 [17] Chirsty, A. A. and Sivarukshy, P., “*Comparison of Adsorption Properties of Commercial Silica and*  
280 *Rice Husk Ash (RHA) Silica: A Study by NIR Spectroscopy*,” *Open Chem.*, 2021, 19, 426–431.
- 281 [18] Emdadi, Z., Asim, N., Yarmo, M. A, Ebadi, M., Mohammad, M. and Sopian, K., “*Chemically*  
282 *Treated Rice Husk Blends as Green Desiccant Materials for Industrial Application*.” *Chem. Eng.*  
283 *Technol.*, 2017, 40, 1619–1629.
- 284 [19] He, S., Chen, G., Xiao, H., Shi, G., Ruan, C., Ma, Y., Dai, H., Yuan, B., Chen, X. and Yang., X.,  
285 “*Facile Preparation of N-Doped Activated Carbon Produced from Rice Husk for CO<sub>2</sub> Capture*.” *J.*  
286 *Colloid Interface Sci.*, 2021, 582, 90–101.
- 287 [20] Shrestha, L., Thapa, M., Shrestha, R., Maji, S., Pradhananga, R. and Ariga, K., “*Rice Husk-Derived*  
288 *High Surface Area Nanoporous Carbon Materials with Excellent Iodine and Methylene Blue*  
289 *Adsorption Properties*.” *C*, 2019, 5, 10.
- 290 [21] Liu, Y., Huo, Z., Song, Z., Zhang, C., Ren, D., Zhong, H. and Jin, F., “*Preparing a Magnetic*  
291 *Activated Carbon with an Expired Beverage as Carbon Source and KOH as The Activator*.” *J.*  
292 *Taiwan Inst. Chem. Eng.*, 2019, 96, 575–587.
- 293 [22] Philia, J., Widayat, W., Sulardjaka, S., Nugroho, G. A. and Darydzaki, A. N., “*Aluminum-Based*  
294 *Activation of Natural Zeolite for Glycerol Steam Reforming*.” *Results Eng.*, 2023, 19, 101247.
- 295 [23] Muslim, A., Purnawan, E., Meilina, H., Azwar, M. Y., Deri, N. O. and Kadri, A., “*Adsorption of*  
296 *Copper Ions onto Rice Husk Activated Carbon Prepared Using Ultrasound Assistance:*  
297 *Optimization Based on Step-by-Step Single Variable Knockout Technique*.” *J. Eng. Sci. Technol.*,  
298 2022, 17, 2496–2511.
- 299 [24] Sun, S., Yu, Q., Li, M., Zhao, H. and Wu, C., “*Preparation of Coffee-Shell Activated Carbon and*  
300 *Its Application for Water Vapor Adsorption*.” *Renew. Energy*, 2019, 142, 11–19.
- 301 [25] Mianowski, A., Owczarek, M. and Marecka, A., “*Surface Area of Activated Carbon Determined by*  
302 *the Iodine Adsorption Number*.” *Energy Sources, Part A: Recovery, Utilization, and Environmental*  
303 *Effects*, 2007, 29, 839–850.



- 304 [26] Linares-Solano, A., Lillo-Ródenas, M. A., Marco-Lozar, J. P., Kunowsky, M. and Romero-Anaya,  
305 A. J., “*Naoh and KOH for Preparing Activated Carbons Used in Energy and Environmental*  
306 *Applications.*” *Int. J. Energy, Environment and Economics*, 2012, 20, 59–91.
- 307 [27] Oginni, O., Singh, K., Oporto, G., Dawson-Andoh, B., McDonald, L. and Sabolsky, E., “*Influence*  
308 *of One-Step and Two-Step KOH Activation on Activated Carbon Characteristics.*” *Bioresour.*  
309 *Technol. Rep.*, 2019, 7, 100266.
- 310 [28] Yang, H. M., Zhang, D. H., Chen, Y., Ran, M. J. and Gu, J. C., “*Study on The Application of KOH*  
311 *to Produce Activated Carbon to Realize the Utilization of Distiller’s Grains.*” *IOP Conf. Ser: Earth*  
312 *Environ. Sci.*, 2017, 69.
- 313 [29] Yu, Q., Zhao, H., Zhao, H., Sun, S., Ji, X., Li, M. and Wang, Y., “*Preparation of Tobacco-Stem*  
314 *Activated Carbon from Using Response Surface Methodology and Its Application for Water Vapor*  
315 *Adsorption in The Solar Drying System.*” *Sol. Energy*, 2019, 177, 324–336.
- 316 [30] Liang, Q., Liu, Y., Chen, M., Ma, L., Yang, B., Li, L. and Liu, Q., “*Optimized Preparation of*  
317 *Activated Carbon from Coconut Shell and Municipal Sludge.*” *Mater. Chem. Phys.*, 2020, 241,  
318 122327.
- 319 [31] Cardenas, C., Farrusseng, D., Daniel, C. and Aubry, R., “*Modeling of Equilibrium Water Vapor*  
320 *Adsorption Isotherms on Activated Carbon, Alumina and Hoplite.*” *Fluid Phase Equilib.*, 2022, 561,  
321 113520.
- 322 [32] Wang, T., Tian, S., Li, G., Sheng, M., Ren, W., Liu, Q., Tan, Y. and Zhang, P., “*Experimental Study*  
323 *of Water Vapor Adsorption Behaviors on Shale.*” *Fuel*, 2019, 248, 168–177.
- 324 [33] Robati, D., “*Pseudo-Second-Order Kinetic Equations for Modelling Adsorption Systems for*  
325 *Removal of Lead Ions Using Multi-Walled Carbon Nanotube.*” *J. Nanostruct. Chem.*, 2013, 3, 55.
- 326